ISSN 0915-633X

NATIONAL INSTITUTE FOR FUSION SCIENCE

Simple Emittance Measurement of H^- Beams from a Large Plasma Source

S.K. Guharay, K. Tsumori, M. Hamabe, Y. Takeiri,
O. Kaneko, T. Kuroda

(Received - Jan. 16, 1996)

NIFS-405 Mar. 1996

RESEARCH REPORT
NIFS Series

NAGOYA, JAPAN

Simple emittance measurement of H^- beams from a large plasma source

S. K. Guharay*, K. Tsumori, M. Hamabe**, Y. Takeiri, O. Kaneko, T. Kuroda

National Institute for Fusion Science
Nagoya 464-01, Japan

Abstract

An emittance meter is developed using pepper-pot method. Kapton foils are used to detect intensity distributions of small beamlets at the "image" plane of the pepper-pot. Emittance of H^- beams from a large plasma source for the neutral beam injector of the Large Helical Device (LHD) has been measured. The normalized emittance (95%) of a 6 mA H^- beam with emission current density of about 10 mA/cm^2 is ~ 0.59 mm mrad. The present system is very simple, and it eliminates many complexities of the existing schemes.

Keywords: H^- beam, neutral beam injector, emittance measurements, pepper-pot method, Kapton foil detector.

*On leave from Institute for Plasma Research, University of Maryland, College Park, Maryland 20742, U.S.A.
**The Graduate University for Advanced Studies, Japan.

Emittance is a figure of merit of charged particle beams. Simply speaking, emittance is a measure of the trace-space area occupied by a distribution of beam particles. The emittance concept and its implications in beam physics have been discussed in numerous articles[1-4]. This parameter relates to many basic problems in researches of current interest, namely, high energy accelerators, ion beam microscopy, electron beams for free electron lasers, etc. In recent times, interests in measuring this parameter and characterizing the ion beams from a source have occurred in magnetic fusion research also. The motivation for generating high-quality ion beams arises due to their demand in the area of neutral beams for additional plasma heating as well as for diagnostics. Several techniques for emittance measurements have been reported in the literature[5-11]. The two common approaches are the slit-and-collector method and the pepper-pot method. Signals in the slit-and-collector method are detected electrically using very sensitive, ultra low-noise current amplifiers. Some drawbacks of this method are circumvented in the slit-and-electric sweep scanner system[7]. Contamination of signals due to noise, secondary electrons, etc., complicates the analysis in the electrical method of detection, especially in the slit-and-collector method. In a pepper-pot emittance meter, an optical method of detection, namely, fluorescence due to particle beams, is normally used. Although the optical schemes are rather inexpensive and relatively less cumbersome, long-term stability of a fluorescent screen (namely, phosphors) and linearity of its response with beam current (or beam power) are issues of concern. Hence, further work for simple, reliable schemes is warranted.

The present article highlights a simple emittance measurement system which has been successfully used to characterize H^- ion beams from a large plasma source. This prototype ion source on the Neutral Beam Injector (NBI) test stand of National Institute for Fusion Science (NIFS) is one-third scaled of the actual source required for the Large Helical Device (LHD) program. The ion

source and the NIFS test stand have been described elsewhere[12-14]. Considering the complex experimental environment for accessibility in the NIFS NBI test stand and also some special characteristics of the H^- ion beams, namely, high beam energy (~ 90 keV), very low beam divergence (~ a few mrad at 1/e folding beam size) and low duty factor (0.003), we have determined that a pepper-pot type emittance meter offers a good solution.

Wang et al.[9] have earlier derived a practical formula for emittance in terms of geometrical parameters of the beam and the pepper-pot system. Assuming the beam to be axisymmetric and the four-dimensional phase-space density distribution bounded by a hyperellipsoid, the full beam emittance ϵ is expressed as

$$\epsilon = (RD/2z)\,(D_z/D - S_z/S)[1 - (S/R)^2]^{-1/2}. \qquad (1)$$

R is the beam radius, D is the diameter of the pepper-pot holes, z is the distance between the pepper pot plane and the detector plane, D_z is the diameter of beamlets at the detector plane, S_z and S correspond, respectively, to the distances of the center of a beamlet from the beam axis at the detector plane and at the pepper-pot plane. The above notations follow ref.9. For the beamlet through the center hole of the pepper-pot, the parameter S = 0 and correspondingly, $S_z = 0$. In this limiting case, S_z/S is taken as 1. Any beam expansion downstream from the pepper-pot plane will be due to emittance only if the dimension of the pepper-pot holes is small enough to ignore space-charge effects of the beamlets. Mathematically speaking, the ratio of the space-charge force to the emittance force, i.e., Ka^2/ϵ^2 must be $<<$ 1. Here, K ($= 2I/I_0\beta^3\gamma^3$, I is the beam current, I_0 is the characteristic current of the beam species, $\beta = v/c$, and γ is the relativistic mass correction factor) is the generalized beam perveance, and a is the radius of the beamlet through the pepper-pot hole.

The experimental arrangement is shown in Fig. 1. The present instrument, as in Fig.2, consists

of a deep Faraday cup in conjunction with a 2D calorimeter array (as indicated in Fig. 1) and a pepper-pot assembly. Here, the most notable point is the use of Kapton foils as detector. The "images" of small pepper-pot holes are automatically monitored by the Kapton foils. The pepper-pot assembly has two essential parts: (1) a plate with multiple holes through which small beamlets emerge, and (2) a Kapton foil where the images due to the small beamlets are captured after their expansion primarily due to the emittance force. In Fig. 3 (a) are shown the pepper-pot holes (12 horizontally, 12 vertically, 12 diagonally, and a center hole) which are drilled very precisely on a 90 mm x 90 mm x 2 mm stainless steel plate. Very uniform and smooth geometry of the holes are obtained by careful drilling and chemical etching. The geometry of the holes on the downstream side of the plate is especially important; the holes are examined by a microscope. The diameter of the holes is 194 μm. A special retainer, as in Fig. 3(b), holds the surface of the 50 μm thick Kapton foil flat. The Kapton foil is held parallel to the pepper-pot plate by precision stainless steel spacers. The front surfaces of the Faraday cup and the pepper-pot plate containing multiple holes lie on the same vertical plane. The calorimeter array consists of copper disks (18 horizontally, 18 vertically, and 1 at the center) and thermocouples in conjunction with each disk. The diameter of the disks is 6 mm, and they are separated by 1 cm. The 2D calorimeter array measures the beam distribution in a single shot. This allows to cross-check the Faraday cup measurements over several shots. Since the aperture of the Faraday cup is 3.2 mm, it can measure the beam distribution with a spatial resolution better than the calorimeter.

The operating conditions of the ion source are set by optimizing the characteristic source parameters, namely, gas pressure, filament current, discharge voltage, discharge current, extraction voltage, and extracted H^- current. Nominal discharge parameters correspond to: gas pressure of

about 8 mTorr, discharge power of about 35 kW, extraction voltage of about 9.4 kV, acceleration voltage of about 79.4 kV, pulse length of about 300 ms, and duty factor of about 0.003. The extracted H^- current is typically about 6 mA giving an emission current density of about 10 mA/cm^2. The source is adjusted mechanically to achieve the beam axis perpendicular to the diagnostics plane. Beam distributions are measured in the two orthogonal planes using the 2D calorimeter array, and the beam axis is evaluated.

The beam emittance is measured at a distance of about 5 meters from the ion source. The pepper-pot assembly is inserted into the vacuum vessel through a top port. A load lock above the top port (Fig.2) isolates the ion source environment, and it allows to perform any preparatory work for the pepper-pot assembly. A precision moveable rod carrying the emittance meter is dropped about 3 meters from the top port of the vacuum vessel so that the beam is intercepted by the Faraday cup. The beam distribution on the plane of the pepper-pot's front surface is measured. Figure 4(a) shows a typical beam distribution using the Faraday cup. The experimental data fit well with a Gaussian distribution. The half width at 1/e level of the peak current density is 2.3 cm. This value matches well with the corresponding result from the intensity contours in Fig. 4(b) measured by the calorimeter array. The beam width of interest (such as, full width, 3σ width, etc.) can be determined from these results, and the appropriate value is used in expression (1) for beam emittance.

Now, the crux of the problem is to measure the "image" of the pepper-pot holes on the Kapton foil. The images formed by the beamlets through the pepper-pot holes carry information about the angular spread of the beam due to emittance. As described earlier, thirty-seven pepper-pot holes are used and their images are captured on the Kapton foil. Fifteen to twenty shots are typically required in the present situation to get good fidelity of the pattern on the Kapton foil. The number

of shots depends essentially on the power density of beamlets at the image plane. Good reproducibility of the shots is a key issue here, and this is ascertained by conditioning of the ion source. The intensity distributions across a few beamlets on the Kapton foil are shown in Fig. 5. A magnified picture of one of the distributions is shown in Fig.6. These results are obtained by scanning the patterns using a densitometer with a resolution of 10 μm. The exposure patterns have been also examined using a microscope with a CCD coupled image intensifier. A typical picture of the beam spot is shown in Fig. 7. The results agree reasonably well with the aformentioned measurements using the densitometer. Two important points are noted in Kapton exposures.

(1) The individual distribution in Fig. 5 is Gaussian-like when the distance between the pepper-pot plate and the Kapton foil is ~ 4.2 cm. For shorter gaps, ≤ 2 cm, when the Kapton foil is very close to the pepper-pot plate, the intensity distribution is found to be hat-like with sharp flat top.

(2) The area covering each intensity distribution seems to follow the same behavior as the current distribution of the beamlets at the pepper pot plane.

The response of the Kapton foil thus seems linear with the incident beam current (for the same beam voltage). Preliminary experiments with Kapton foils were done earlier in the context of high energy (~ 150 keV) Ar^+ ion beams[15].

Finally, the emittance of the aforementioned beam is estimated. The emittance of a certain beam fraction, say, 95% is of practical interest. If the beam boundary is considered to be extended up to 5% of the peak intensity level, the corresponding beam radius R is about 4.2 cm, and we obtain D_z = 294 μm from Fig. 6. Since the pepper-pot holes are very small (diameter = 194 μm), space-charge effects do not play any significant role in determining the "image" patterns on the Kapton foil; the enhancement of the beamlet (or the "image") size, D_z, is primarily due to the emittance force. The

value of S_z is observed to be very close to S for all beamlets. This is due to the fact that the divergence of the beam at the pepper-pot plane is very small, ~ 6 mrad at 1/e- folding beam radius of about 2.3 cm. This yields an inappreciably small value of the local beam divergence over the dimension of the pepper-pot holes. Therefore, the deflection of the beam axis across a gap of 4.2 cm between the pepper-pot plate and the Kapton foil is negligible. So, we have used $S_z/S \approx 1$ in our experiment. Plugging in the above values in expression (1), we obtain the 95% beam emittance as about 50.0 mm mrad. Note that the usual factor of π is not included here as the trace-space area is $\pi\epsilon$. The analysis, so far, is based on the study of a beamlet through one particular hole. As a large number of beamlets are imaged on the Kapton foil, we can achieve good statistics of the data. Analyzing the data set of the intensity distributions in Fig.5 we obtain ϵ (95%) = 43.2 ± 6.4 mm mrad. The normalized emittance of the beam is defined as $\epsilon_n = \beta\gamma\epsilon$. Hence, in the present case, the normalized emittance is estimated as ϵ_n (95%) = 0.59 mm mrad.

In conclusion, the present apparatus has been adapted easily and reliably to measure the emittance of H^- beams relevant to the neutral beam programs for magnetic fusion. The evidence for linearity of response and good sensitivity of the detection system using Kapton foils attributes its strong merits. The present detection scheme avoids any complexity of the usual two-step processes in an optical method, namely, first, capturing pictures from a luminescent screen and second, processing the image patterns. The current method is direct, and it displays the exposure patterns automatically. This method appears to be particularly useful in a complex environment where the view ports are restricted. We have made preliminary measurements with this emittance meter to investigate the dependence of beam emittance on characteristic parameters, namely, gas pressure, cesium feed, etc. The results are beyond the scope of this article, and they will be reported elsewhere.

Acknowledgments

One of the authors (S.K.G.) thankfully acknowledges the support of the Ministry of Education and Culture (Monbusho), Japan for offering Guest Professorship. Also, he thanks Professor A. Iyoshi for the privilege to work at the National Institute for Fusion Science, Nagoya, and Dr. A. Ando of Tohoku University and Dr. R. Keller of Lawrence Berkeley Laboratory for many helpful discussions. Valuable help of Mr. K. Mizusawa and T. Kawamoto is thankfully acknowledged.

References:

1. J. D. Lawson, in High-Brightness Beams for Advanced Accelerator Applications, AIP Conf. Proc. No. 253, ed. W. W. Destler and S. K. Guharay (American Institute of Physics, N.Y.) 1992, p. 1.

2. C. Lejeune and J. Aubert, in Advances in Electronics and Electron Physics, Supplement 13A (Academic Press) 1980, p. 159.

3. T. Wangler, Proceedings of the 8th ICFA Advanced Beam Dynamics Workshop on Space-Chrage Dominated Beams and Applications of High Brightnesss Beams, Bloomington, IN, Oct. 10- 13, 1995 (To be published).

4. M. Reiser, Theory and Design of Charged Particle Beams (John Wiley & Sons, Inc., N.Y.), 1994, chapter 3.

5. A. Van Steenbergen, Nucl. Instrum. & Methods **51**, 245 (1967).

6. G. Riehl, J. Pozimski, W. Barth, Proc. Linear Accelerator Conf., Albuquerque, New Mexico, Sept. 10-14, 1990, p. 755.

7. P. W. Allison, J. D. Sherman, D. B. Holtkamp, IEEE Transac. Nuclear Science, **NS-30**, 2204 (1983).

8. B. Strongin and A. Salop, Proc. Linear Accelerator Conf., Albuquerque, New Mexico, Sept. 10-14, 1990, p. 758.

9. J. G. Wang, D. X. Wang, M. Reiser, Nucl. Instrum. and Methods in Phys. Res. **A307**, 190 (1991).

10. J. Peters, Rev. Sci. Instrum. **65**, 1459 (1994).

11.T. Shirai, H. Dewa, H. Fujita, M. Kando, M. Ikegami, Y. Iwashita, S. Kakigi, A. Noda, M. Inoue, Proc. Linear Accelerator Conf., Tsukaba, Japan, August 21-26, 1994, p. 908.

12. A. Ando, K. Tsumori, et al., Phys. Plasmas **1**, 2813 (1994).

13. K. Tsumori, A. Ando, et al., Fusion Engineering and Design **26**, 473 (1995).

14. O. Kaneko, A. Ando, Y. Oka, Y. Takeiri, K. Tsumori, R. Akiyama, T. Kawamoto, T. Kurata, K. Mineo, and T. Kuroda, Proc. 17th Symp. on Fusion Technology, vol. 1, p. 544.

15. R. Keller, private communication.

Figure Captions:

Fig. 1 Schematic diagram of the experimental arrangement.

Fig. 2 Schematic of the emittance meter system.

Fig. 3 (a) Pepper-pot holes, and (b) Kapton foil holder.

Fig. 4 (a) H^- current density distribution using a deep Faraday cup, and (b) H intensity contours measured by a calorimeter array. The contours are mapped at an intensity interval of 10%.

Fig. 5 Intensity distributions across 7 beamlets on the Kapton foil. The center of the beamlets are spaced at an interval of 4 mm. The actual horizontal scale is revealed clearly in Fig. 6.

Fig.6 An enlarged display of a typical intensity distribution.

Fig. 7 Picture of a beam spot on the Kapton foil using a microscope with an image intensifier. The red color contrasts the exposed area against the background in yellow.

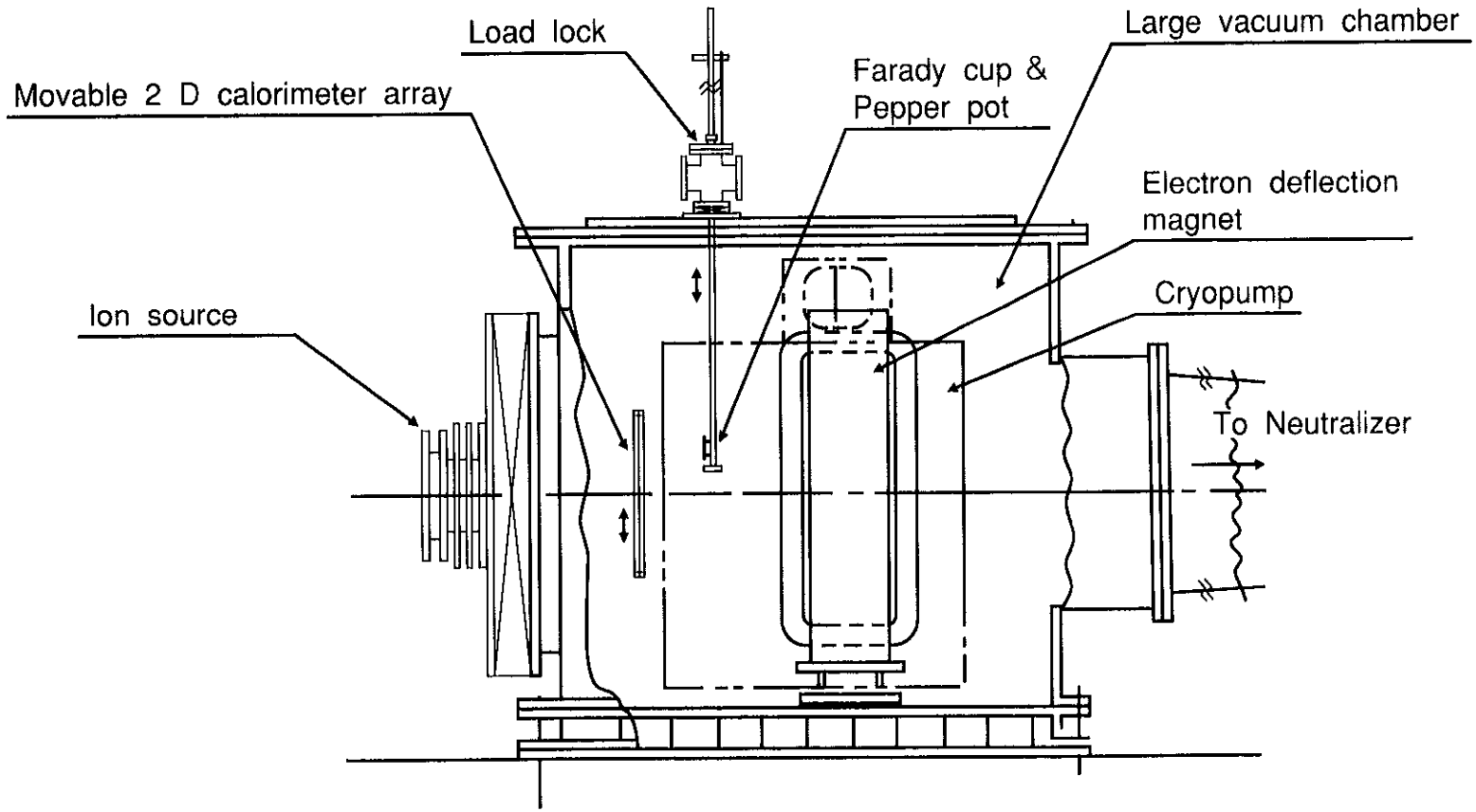
Load lock
Large vacuum chamber
Movable 2 D calorimeter array
Farady cup &
Pepper pot
Electron deflection
magnet
Cryopump
Ion source
To Neutralizer

Fig. 1

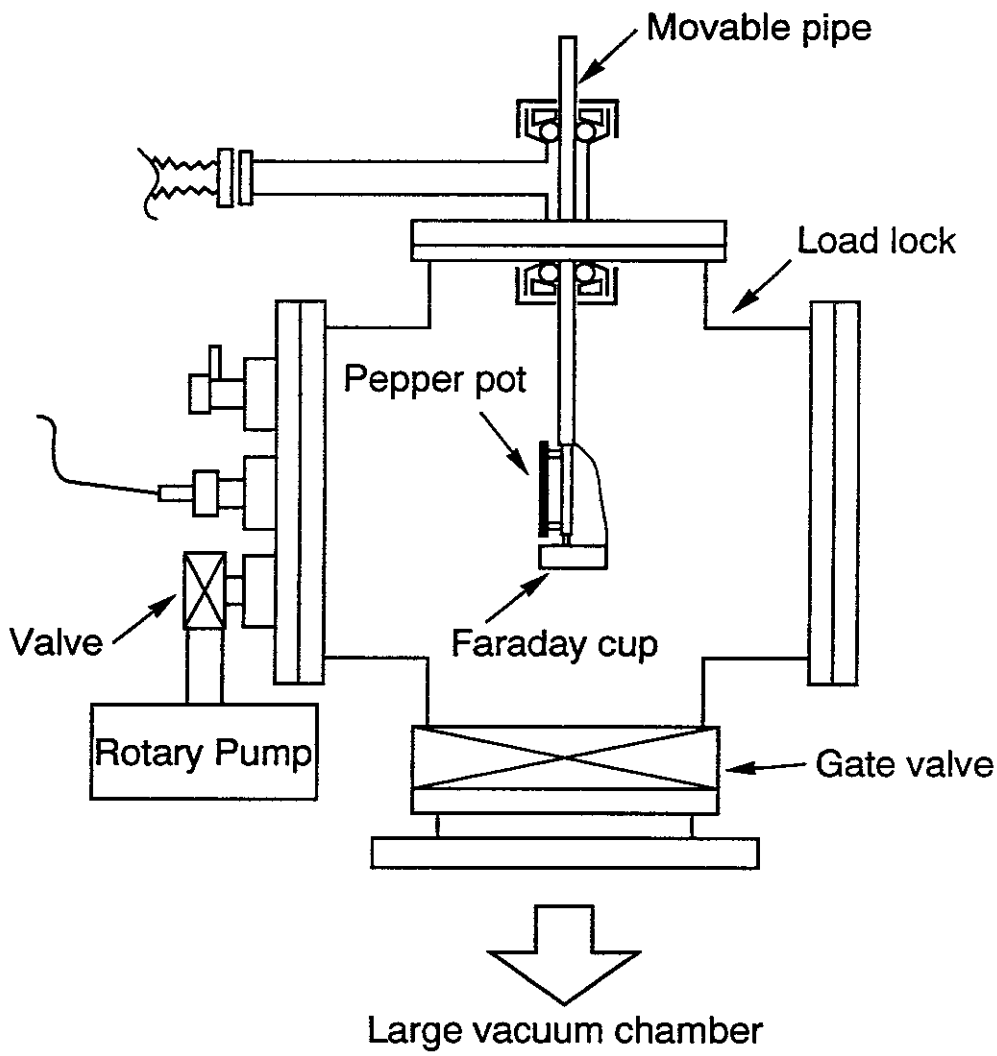
Movable pipe
Load lock
Pepper pot
Valve
Faraday cup
Rotary Pump
Gate valve
Large vacuum chamber

Fig. 2

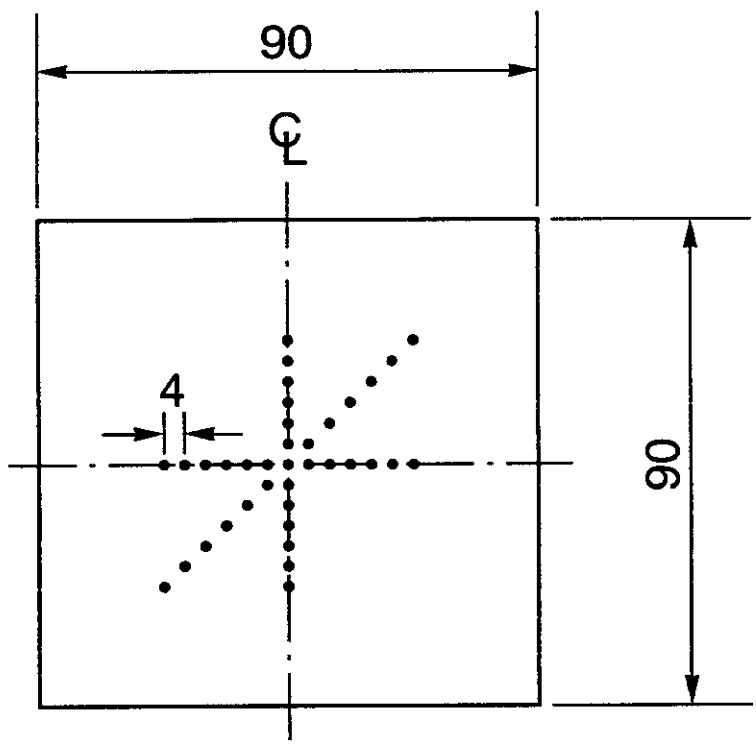

Fig. 3 (a)

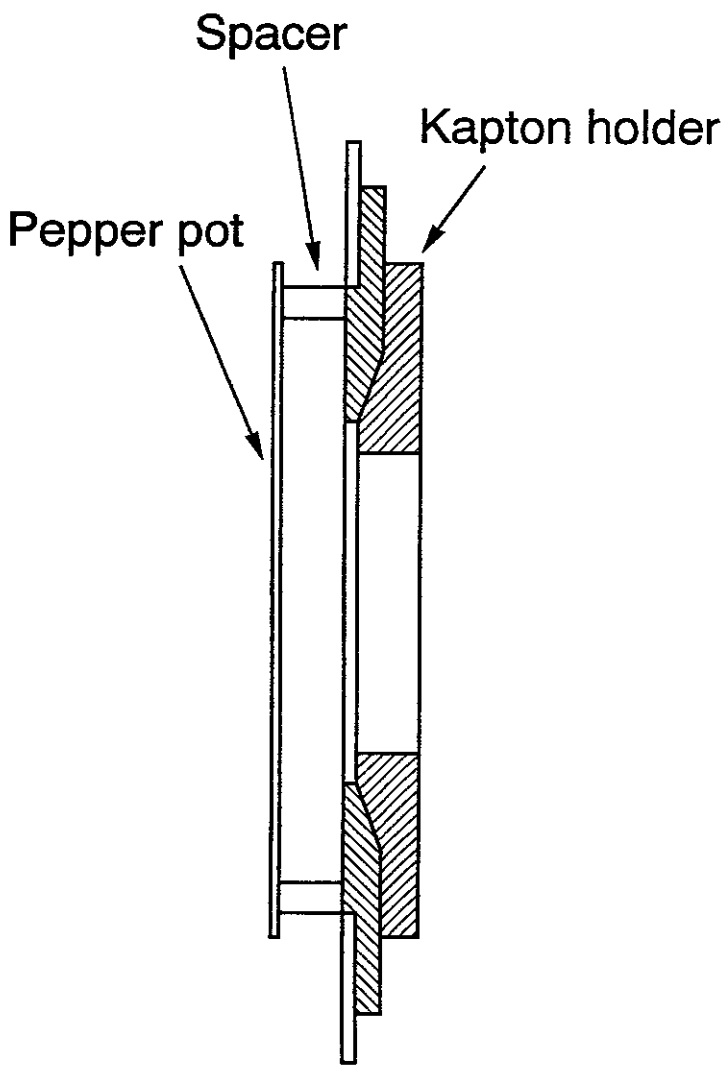

Fig. 3 (b)

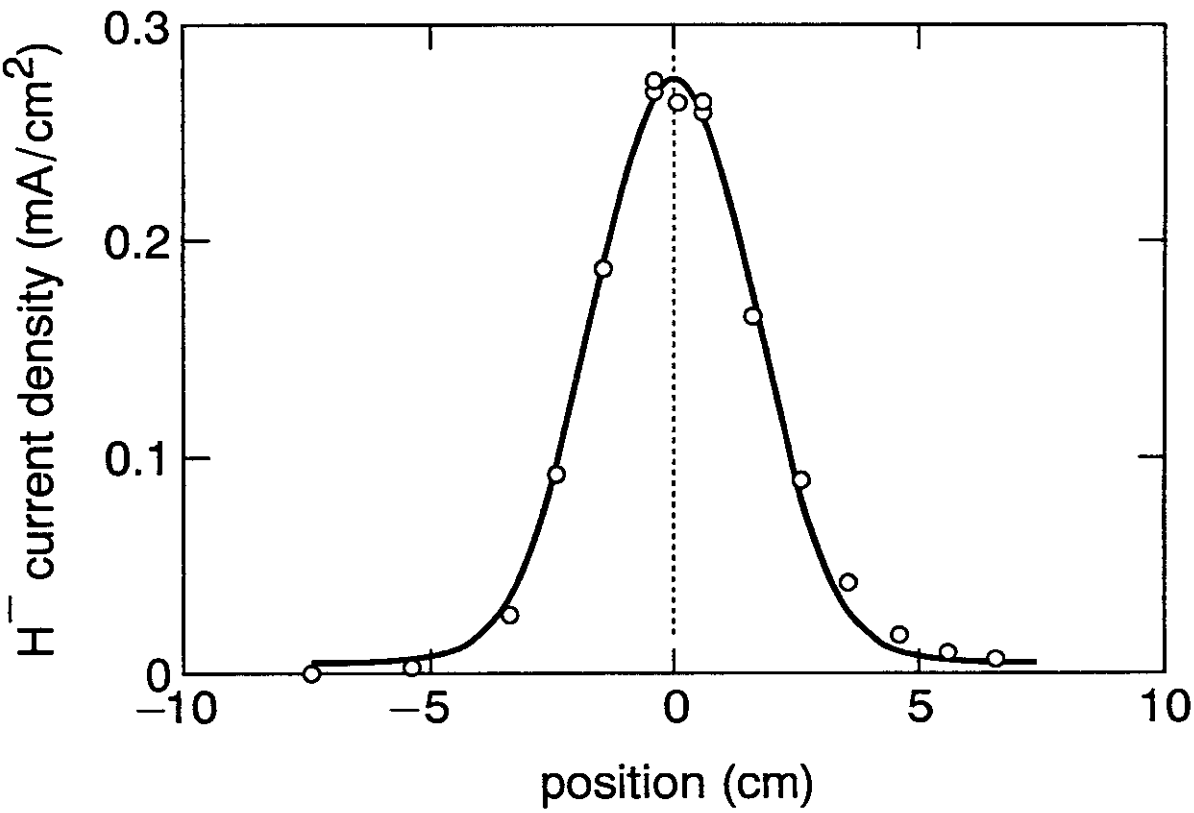

Fig. 4 (a)

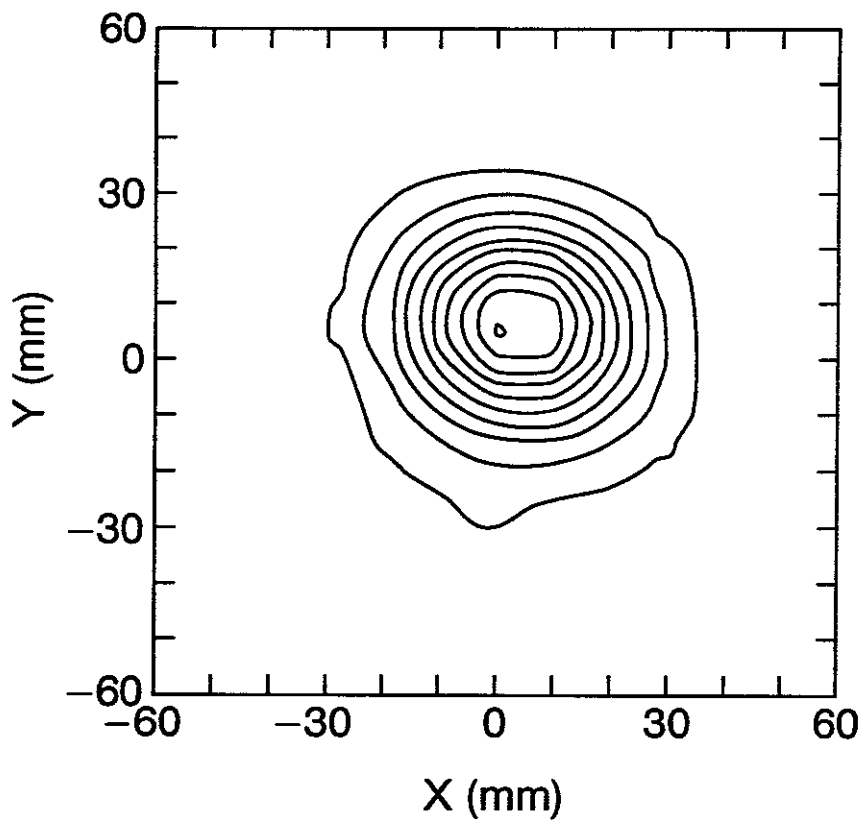

Fig. 4 (b)

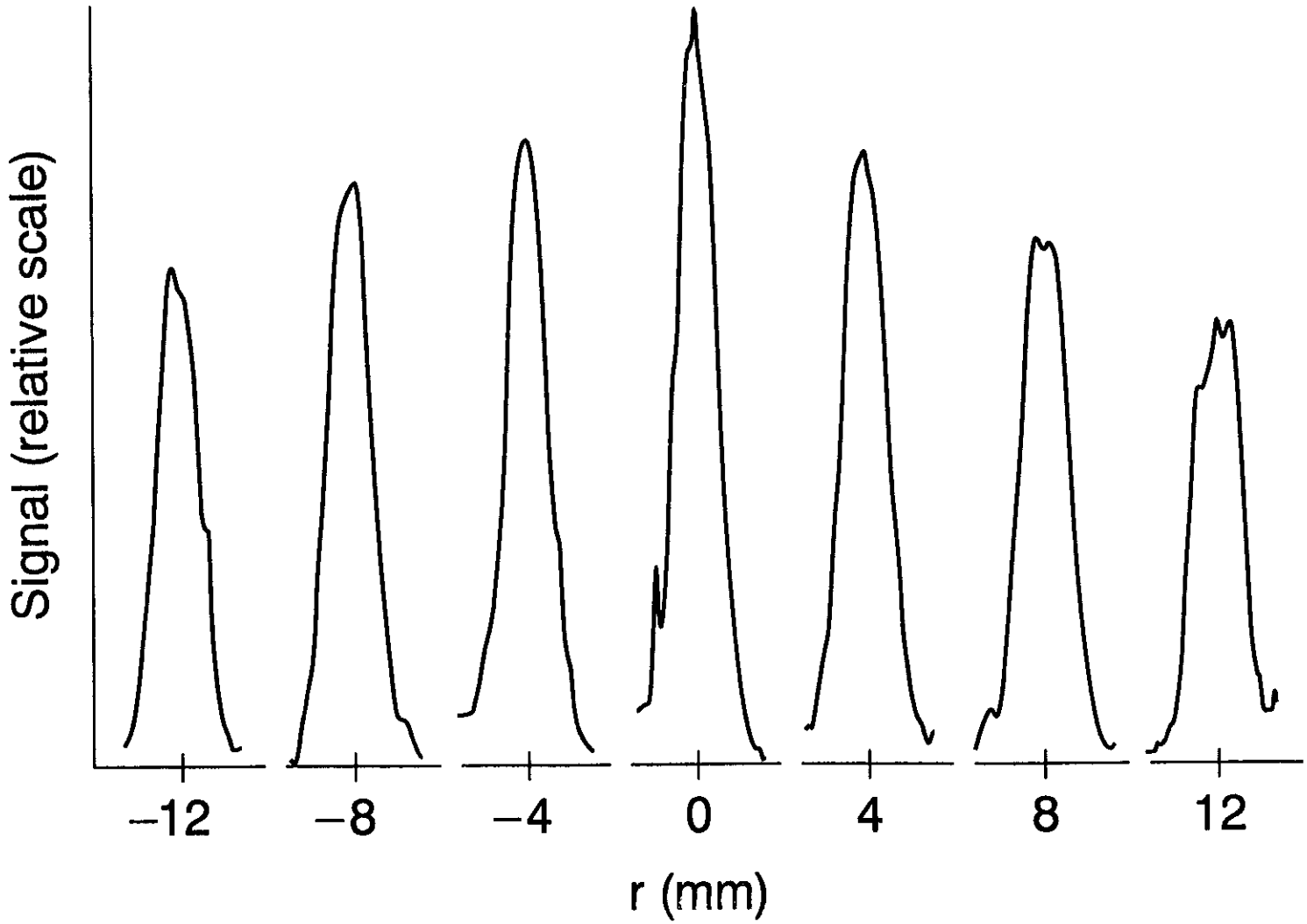

Fig. 5

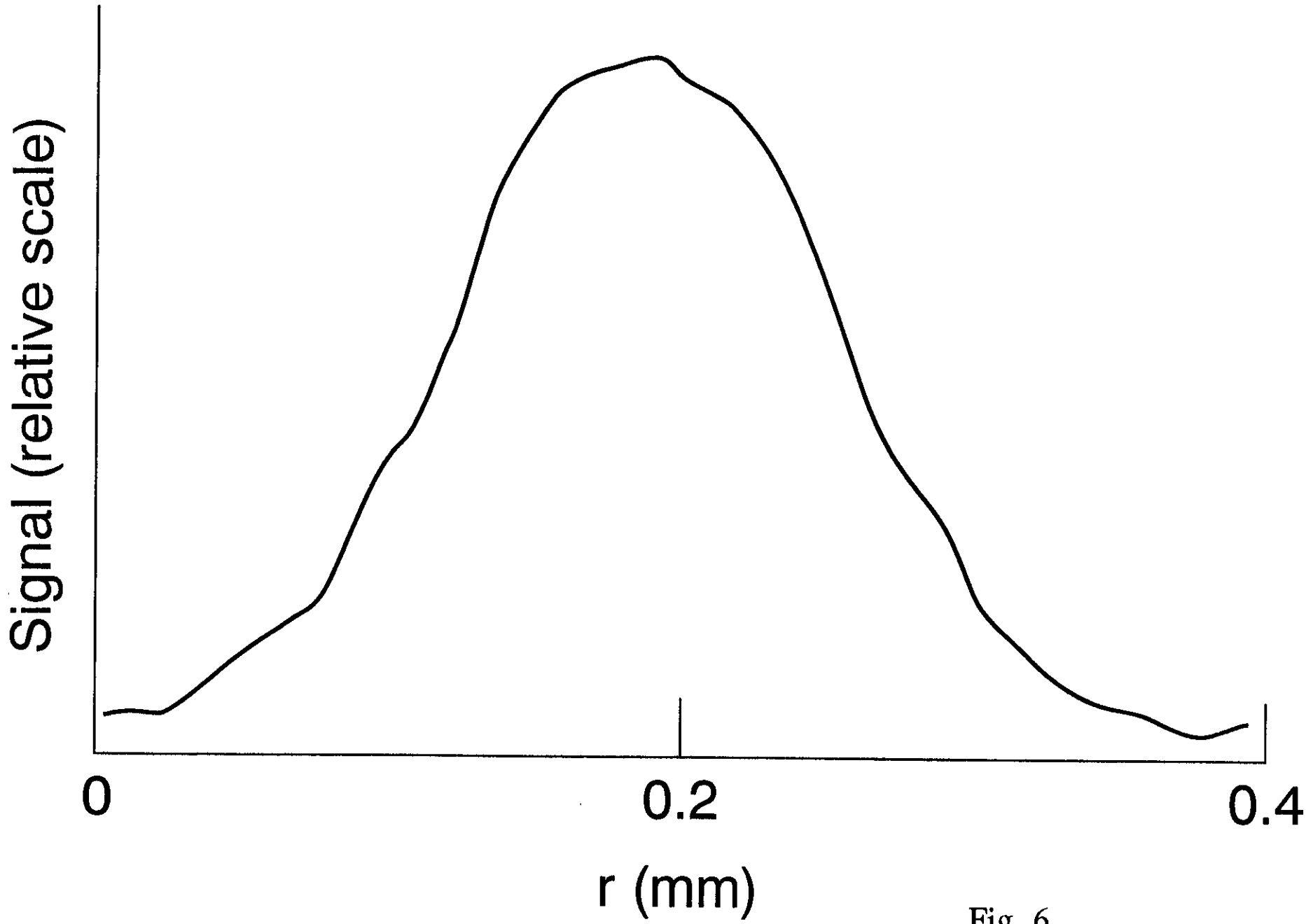

Fig. 6

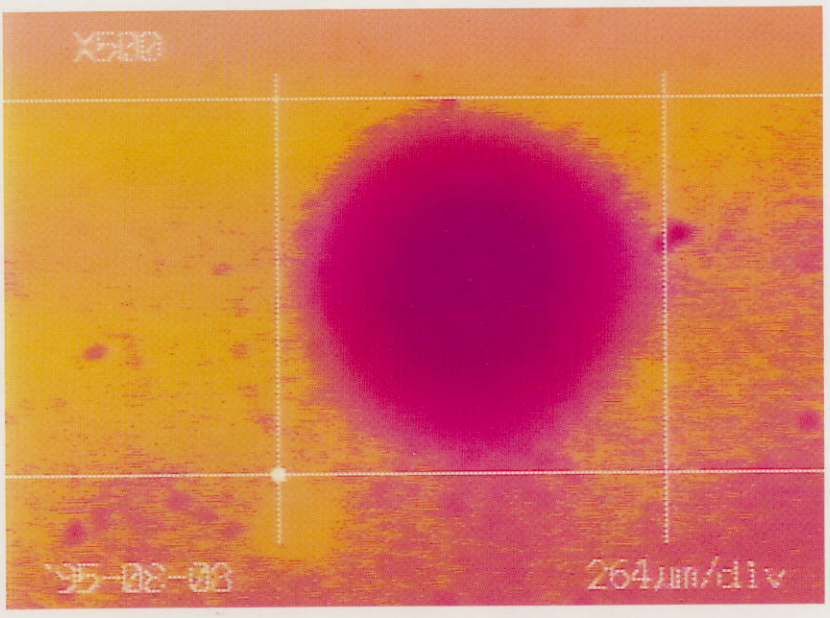

Fig. 7

Recent Issues of NIFS Series

NIFS-358 M. Ida and T. Yabe,
Implicit CIP (Cubic-Interpolated Propagation) Method in One Dimension; May 1995

NIFS-359 A. Kageyama, T. Sato and The Complexity Simulation Group,
Computer Has Solved A Historical Puzzle: Generation of Earth's Dipole Field; June 1995

NIFS-360 K. Itoh, S.-I. Itoh, M. Yagi and A. Fukuyama,
Dynamic Structure in Self-Sustained Turbulence; June 1995

NIFS-361 K. Kamada, H. Kinoshita and H. Takahashi,
Anomalous Heat Evolution of Deuteron Implanted Al on Electron Bombardment; June 1995

NIFS-362 V.D. Pustovitov,
Suppression of Pfirsch-schlüter Current by Vertical Magnetic Field in Stellarators; June 1995

NIFS-363 A. Ida, H. Sanuki and J. Todoroki
An Extended K-dV Equation for Nonlinear Magnetosonic Wave in a Multi-Ion Plasma; June 1995

NIFS-364 H. Sugama and W. Horton
Entropy Production and Onsager Symmetry in Neoclassical Transport Processes of Toroidal Plasmas; July 1995

NIFS-365 K. Itoh, S.-I. Itoh, A. Fukuyama and M. Yagi,
On the Minimum Circulating Power of Steady State Tokamaks; July 1995

NIFS-366 K. Itoh and Sanae-I. Itoh,
The Role of Electric Field in Confinement; July 1995

NIFS-367 F. Xiao and T. Yabe,
A Rational Function Based Scheme for Solving Advection Equation; July 1995

NIFS-368 Y. Takeiri, O. Kaneko, Y. Oka, K. Tsumori, E. Asano, R. Akiyama, T. Kawamoto and T. Kuroda,
Multi-Beamlet Focusing of Intense Negative Ion Beams by Aperture Displacement Technique; Aug. 1995

NIFS-369 A. Ando, Y. Takeiri, O. Kaneko, Y. Oka, K. Tsumori, E. Asano, T. Kawamoto, R. Akiyama and T. Kuroda,
Experiments of an Intense H- Ion Beam Acceleration; Aug. 1995

NIFS-370 M. Sasao, A. Taniike, I. Nomura, M. Wada, H. Yamaoka and M. Sato, *Development of Diagnostic Beams for Alpha Particle Measurement on ITER*; Aug. 1995

NIFS-371 S. Yamaguchi, J. Yamamoto and O. Motojima; *A New Cable -in conduit Conductor Magnet with Insulated Strands*; Sep. 1995

NIFS-372 H. Miura, *Enstrophy Generation in a Shock-Dominated Turbulence*; Sep. 1995

NIFS-373 M. Natsir, A. Sagara, K. Tsuzuki, B. Tsuchiya, Y. Hasegawa, O. Motojima, *Control of Discharge Conditions to Reduce Hydrogen Content in Low Z Films Produced with DC Glow;* Sep. 1995

NIFS-374 K. Tsuzuki, M. Natsir, N. Inoue, A. Sagara, N. Noda, O. Motojima, T. Mochizuki, I. Fujita, T. Hino and T. Yamashina, *Behavior of Hydrogen Atoms in Boron Films during H_2 and He Glow Discharge and Thermal Desorption;* Sep. 1995

NIFS-375 U. Stroth, M. Murakami, R.A. Dory, H. Yamada, S. Okamura, F. Sano and T. Obiki, *Energy Confinement Scaling from the International Stellarator Database*; Sep. 1995

NIFS-376 S. Bazdenkov, T. Sato, K. Watanabe and The Complexity Simulation Group, *Multi-Scale Semi-Ideal Magnetohydrodynamics of a Tokamak Plasma;* Sep. 1995

NIFS-377 J. Uramoto, *Extraction of Negative Pionlike Particles from a H2 or D2 Gas Discharge Plasma in Magnetic Field;* Sep. 1995

NIFS-378 K. Akaishi, *Theoretical Consideration for the Outgassing Characteristics of an Unbaked Vacuum System*; Oct. 1995

NIFS-379 H. Shimazu, S. Machida and M. Tanaka, *Macro-Particle Simulation of Collisionless Parallel Shocks*; Oct. 1995

NIFS-380 N. Kondo and Y. Kondoh, *Eigenfunction Spectrum Analysis for Self-organization in Dissipative Solitons;* Oct. 1995

NIFS-381 Y. Kondoh, M. Yoshizawa, A. Nakano and T. Yabe, *Self-organization of Two-dimensional Incompressible Viscous Flow in a Friction-free Box;* Oct. 1995

NIFS-382 Y.N. Nejoh and H. Sanuki,

The Effects of the Beam and Ion Temperatures on Ion-Acoustic Waves in an Electron Beam-Plasma System; Oct. 1995

NIFS-383 K. Ichiguchi, O. Motojima, K. Yamazaki, N. Nakajima and M. Okamoto
Flexibility of LHD Configuration with Multi-Layer Helical Coils; Nov. 1995

NIFS-384 D. Biskamp, E. Schwarz and J.F. Drake,
Two-dimensional Electron Magnetohydrodynamic Turbulence; Nov. 1995

NIFS-385 H. Kitabata, T. Hayashi, T. Sato and Complexity Simulation Group,
Impulsive Nature in Collisional Driven Reconnection; Nov. 1995

NIFS-386 Y. Katoh, T. Muroga, A. Kohyama, R.E. Stoller, C. Namba and O. Motojima,
Rate Theory Modeling of Defect Evolution under Cascade Damage Conditions:The Influence of Vacancy-type Cascade Remnants and Application to the Defect Production Chracterization by Microstructural Analysis; Nov. 1995

NIFS-387 K. Araki, S. Yanase and J. Mizushima,
Symmetry Breaking by Differential Rotation and Saddle-node Bifurcation of the Thermal Convection in a Spherical Shell; Dec. 1995

NIFS-388 V.D. Pustovitov,
Control of Pfirsch-Schlüter Current by External Poloidal Magnetic Field in Conventional Stellarators: Dec. 1995

NIFS-389 K. Akaishi,
On the Outgassing Rate Versus Time Characteristics in the Pump-down of an Unbaked Vacuum System; Dec. 1995

NIFS-390 K.N. Sato, S. Murakami, N. Nakajima, K. Itoh,
Possibility of Simulation Experiments for Fast Particle Physics in Large Helical Device (LHD); Dec. 1995

NIFS-391 W.X.Wang, M. Okamoto, N. Nakajima, S. Murakami and N. Ohyabu,
A Monte Carlo Simulation Model for the Steady-State Plasma in the Scrape-off Layer; Dec. 1995

NIFS-392 Shao-ping Zhu, R. Horiuchi, T. Sato and The Complexity Simulation Group,
Self-organization Process of a Magnetohydrodynamic Plasma in the Presence of Thermal Conduction; Dec. 1995

NIFS-393 M. Ozaki, T. Sato, R. Horiuchi and the Complexity Simulation Group
Electromagnetic Instability and Anomalous Resistivity in a Magnetic Neutral Sheet; Dec. 1995

NIFS-394 K. Itoh, S.-I Itoh, M. Yagi and A. Fukuyama,

Subcritical Excitation of Plasma Turbulence; Jan. 1996

NIFS-395 H. Sugama and M. Okamoto, W. Horton and M. Wakatani,
Transport Processes and Entropy Production in Toroidal Plasmas with Gyrokinetic Eletromagnetic Turbulence; Jan. 1996

NIFS-396 T. Kato, T. Fujiwara and Y. Hanaoka,
X-ray Spectral Analysis of Yohkoh BCS Data on Sep. 6 1992 Flares - Blue Shift Component and Ion Abundances -; Feb. 1996

NIFS-397 H. Kuramoto, N. Hiraki, S. Moriyama, K. Toi, K. Sato, K. Narihara, A. Ejiri, T. Seki and JIPP T-IIU Group,
Measurement of the Poloidal Magnetic Field Profile with High Time Resolution Zeeman Polarimeter in the JIPP T-IIU Tokamak; Feb. 1996

NIFS-398 J.F. Wang, T. Amano, Y. Ogawa, N. Inoue,
Simulation of Burning Plasma Dynamics in ITER; Feb. 1996

NIFS-399 K. Itoh, S-I. Itoh, A. Fukuyama and M. Yagi,
Theory of Self-Sustained Turbulence in Confined Plasmas; Feb. 1996

NIFS-400 J. Uramoto,
A Detection Method of Negative Pionlike Particles from a H2 Gas Descharge Plasma; Feb. 1996

NIFS-401 K.Ida, J.Xu, K.N.Sato, H.Sakakita and JIPP TII-U group,
Fast Charge Exchange Spectroscopy Using a Fabry-Perot Spectrometer in the JIPP TII-U Tokamak; Feb. 1996

NIFS-402 T. Amano,
Passive Shut-Down of ITER Plasma by Be Evaporation; Feb. 1996

NIFS-403 K. Orito,
A New Variable Transformation Technique for the Nonlinear Drift Vortex; Feb. 1996

NIFS-404 T. Oike, K. Kitachi, S. Ohdachi, K. Toi, S. Sakakibara, S. Morita, T. Morisaki, H. Suzuki, S. Okamura, K. Matsuoka and CHS group;
Measurement of Magnetic Field Fluctuations near Plasma Edge with Movable Magnetic Probe Array in the CHS Heliotron/Torsatron; Mar. 1996

NIFS-405 S.K. Guharay, K. Tsumori, M. Hamabe, Y. Takeiri, O. Kaneko, T. Kuroda,
Simple Emittance Measurement of H- Beams from a Large Plasma Source; Mar. 1996